

Observation of the prominence cavity region using slitless eclipse flash spectra and space borne EUV filtergrams

Cyrille Bazin^{1,2}, Serge Koutchmy¹, Philippe Lamy², and Ehsan Tavabi³

¹IAP, CNRS-UMR 7095 -UPMC, 98 bis Bd Arago 75014 Paris, France
email: bazin@iap.fr; koutchmy@iap.fr

²LAM, CNRS-UMR 6110 -AMU, Pole de l'Etoile, 38 Rue Joliot Curie 13388 Marseille, France
email: philippe.lamy@oamp.fr ³Payame Noor University of Tehran, 14155-6466, I.R. of Iran
email: etavabi@gmail.com

Abstract. We used total solar eclipse free of parasitic light for studying the prominence to corona interface, and the corresponding cavity in the context of the coronal physics. We analysed the visible continuum between the prominences to directly look at the electron density. We demonstrate some enhanced heating in the cavity region. Some similarities with the interface regions are shown: the photosphere to the chromosphere and the prominence to the corona interface. The optically thin neutral Helium at 4713 Å and the singly ionized Helium 4686 Å Paschen α lines are considered. We summed 80 slitless visible eclipse flash spectra that we compare with simultaneously obtained EUV SWAP/Proba2 174 Å images of ESA and AIA/SDO 171Å 193 Å 304 Å and 131 Å filtergrams. Intensity profiles in a radial direction are studied. We deduce the variation of the intensity ratio $I(\text{He I } 4713) / I(\text{He II } 4686)$. Discussion: the temperature rises at the edge of the prominences. We evaluate for the first time with spectrophotometric accuracy the continuum modulations in prominence spectra. W-L intensity deficits are observed near the prominence boundaries in both eclipse spectra and in EUV images, confirming that the prominence -cavity regions correspond to a relative depression of plasma density of the surrounding corona. Conclusion: we demonstrate some enhanced heating occurring in these regions assuming hydrostatic equilibrium.

Keywords. flash spectra, corona, prominence, cavity, EUV lines, He lines

1. Introduction

We take advantage of the occultation of the Sun by the Moon to analyse the low layers of the solar atmosphere at different heights without parasitic light (since the occultation takes place in space). Eclipse slitless flash spectra were obtained during the second contact, just before the totality of the solar eclipse of 11 July 2010 observed in French Polynesia. We used the grating objective technique and fast CCD imaging (see Bazin, Koutchmy and Tavabi 2012). The motivations are to try to explain some similarities between the high First Ionisation Potential- FIP of helium lines intensity ratio in the Chromosphere-Corona Interface CCI and the Prominence to Corona Interface PCI. The low FIP of the faint metallic emission lines and the helium shells above the solar limb are considered in Bazin and Koutchmy (2013). We discuss the importance of the prominence continuum. The optically thin helium line emissions (He I 4713 Å and He II 4686 Å) occurring at total solar eclipses were already analysed using slit spectrograph by Hirayama and Irie (1984). Simultaneous space borne SDO/AIA images (free of seeing effects), described in Cheimets *et al.*(2009) are now additionally used.

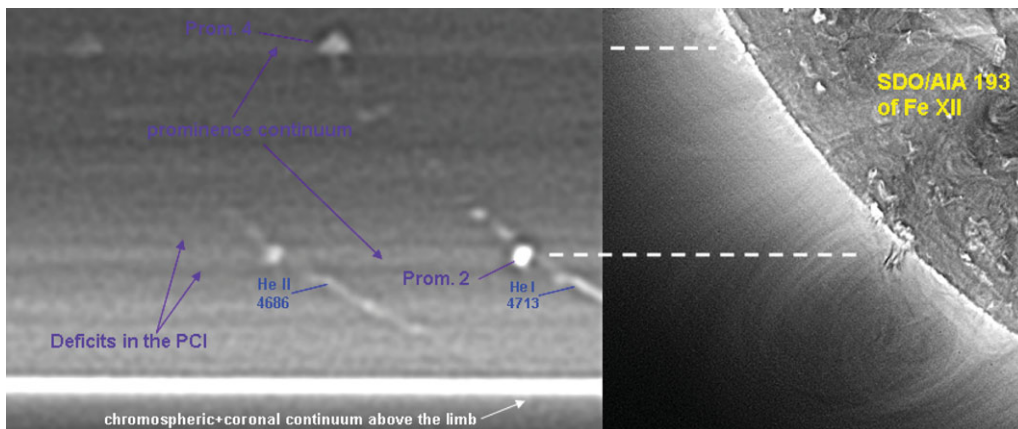


Figure 1. Simultaneous observations of the prominences using the 2010 eclipse flash spectra (left panel) and an image of 12 stacked EUV filtergrams (right panel). The left panel presents the sum of 80 individual flash spectra. The spatial dispersion runs along the horizontal direction and extends over $\approx 65 \text{ \AA}$. The field-of-view along the vertical direction extends over 300 Mm. The prominence studied here labeled 2 is highlighted by its main helium 4713 \AA and 4686 \AA emission lines and its continuum as well as the deficit at the interface between the prominence and the corona. The bright horizontal band near the bottom of the figure is not an artefact but corresponds to the intense chromospheric and coronal continuum above the limb. The right panel presents the summed image at 193 \AA (Fe XII emission at a temperature of 1.5 MK) showing the same prominence 2 in absorption (note also spicules seen in absorption).

2. Observation and data analysis

We summed twelve Fe XII 193 \AA images taken around the time of the eclipse for improving the signal to noise ratio. Figure 1 shows the comparison between the prominences 2 and 4 seen in He I 4713 \AA and He II 4686 \AA lines from the 80 summed flash spectra and the prominence 2 seen in absorption with the surrounding cavity using the SDO/AIA Fe XII 193 \AA 1.5 MK temperature coronal line.

2.1. Helium flash spectra

We then removed the coronal background continuum to obtain the true intensity ratio of He II 4686 \AA / He I 4713 \AA with the radial distance. Figure 2 shows the resulting values. A comparable analysis was recently done in Labrosse *et al.* (2011) for the He II 256 \AA EUV line which is unfortunately blended like the He II 304 \AA line is.

The intensity ratio of He II/He I at heights from 0 to 3 Mm shows a more than 2 times increase (see Figure 2). The same behaviour is seen in the CCI as in the PCI at heights starting from 4 Mm to 22 Mm. In both cases, a dynamic state is observed at small scale, often attributed in the past, to a turbulent effect. These results allow to diagnose the helium shell structuration and the contribution of high FIP elements in these regions.

2.2. EUV filtergrams

The image in the Fe XII 193 \AA line suggests some twisted channels seen in absorption corresponding to the core of the prominence 2. The surrounding cavity shows plasma deficits, see Figure 1 at right. Intensity radial cuts taken along and outside the cavity region in 193 \AA are plotted in Figure 3 for evaluating the scale height using second order and first order exponential decays that fitted the radial profiles along and outside the cavity, respectively. The plasma deficit in the PCI could be associated with some higher temperature (assuming hydrostatic equilibrium), because of the rather low radial gradient

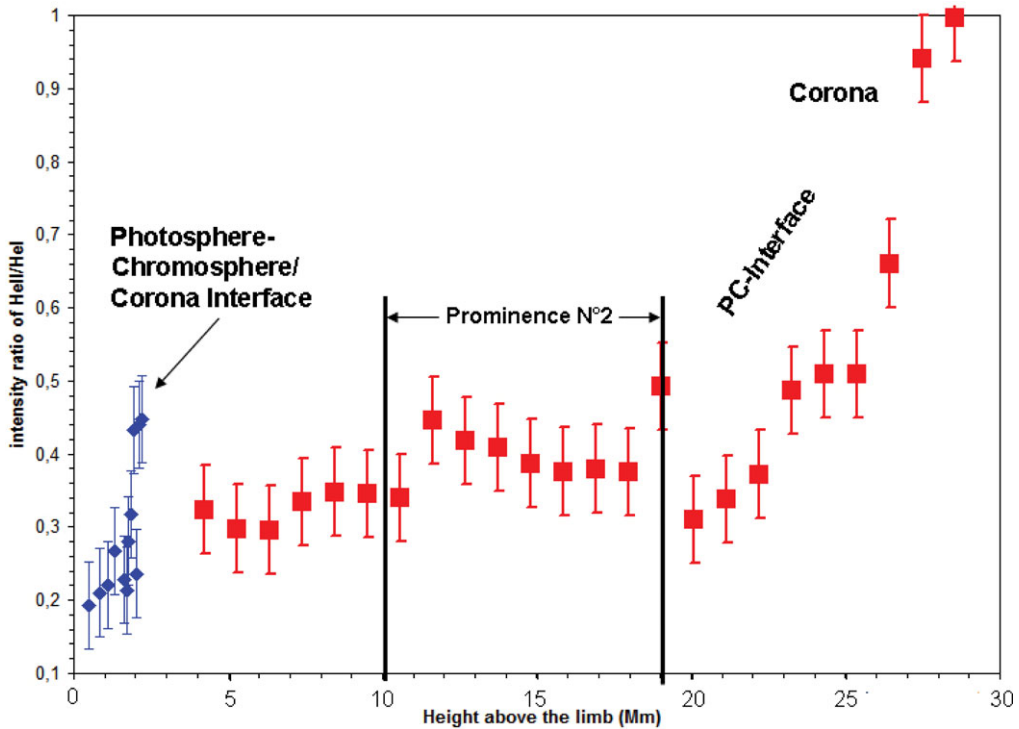


Figure 2. Intensity ratio measurements of the He II 4686 Å / He I 4713 Å as function of the radial distance starting above the limb and upwards to a prominence from eclipse flash spectra. The error bars correspond to one sigma standard deviation, after the coronal continuum background was removed. The losanges correspond to lower altitudes where the crescents of helium lines emissions are recorded, and squares indicate the higher altitudes prominence values.

of densities around and above this prominence. We found $I(h) = 1224 \cdot \exp(-h/18.7) + 454 \cdot \exp(-h/227.4)$, where h is in Mm, along the cavity and $I'(h) = 1724 \cdot \exp(-h/36.1) + 23.5$ outside the cavity. The intensity distribution expressed by the Differential Emission Measure will be more extensively discussed in a forthcoming paper.

3. Discussion

The plots in figure 2 show approximately the same intensity ratio values around 0.4 for both the solar CCI in the lower altitudes, where the gravity could still dominate, and in the PCI at higher altitudes, where the more extended magnetic field dominates. The β of the plasma is low. The continuum in the prominence spectra indicates Thomson scattering from electrons, and possibly a Paschen continuum contribution in denser parts, see Vial *et al.* (1992). The "cold" plasma of the prominence core where the gravity is negligible is surrounded by the hot corona seen in emission of EUV lines. One proposed mechanism responsible of the ionisation of the optically thin He II 4686 Å $P\alpha$ line is the photo-ionisation process by photons coming from the corona like the EUV lines of Fe XII and hotter ones. Because of the rather low radial gradients of densities around the prominence suggesting high temperature when hydrostatic equilibrium is assumed, the plasma deficit could be associated with some enhanced heating. Figure 3 points the slopes taken on radial cuts along and outside the cavity region.

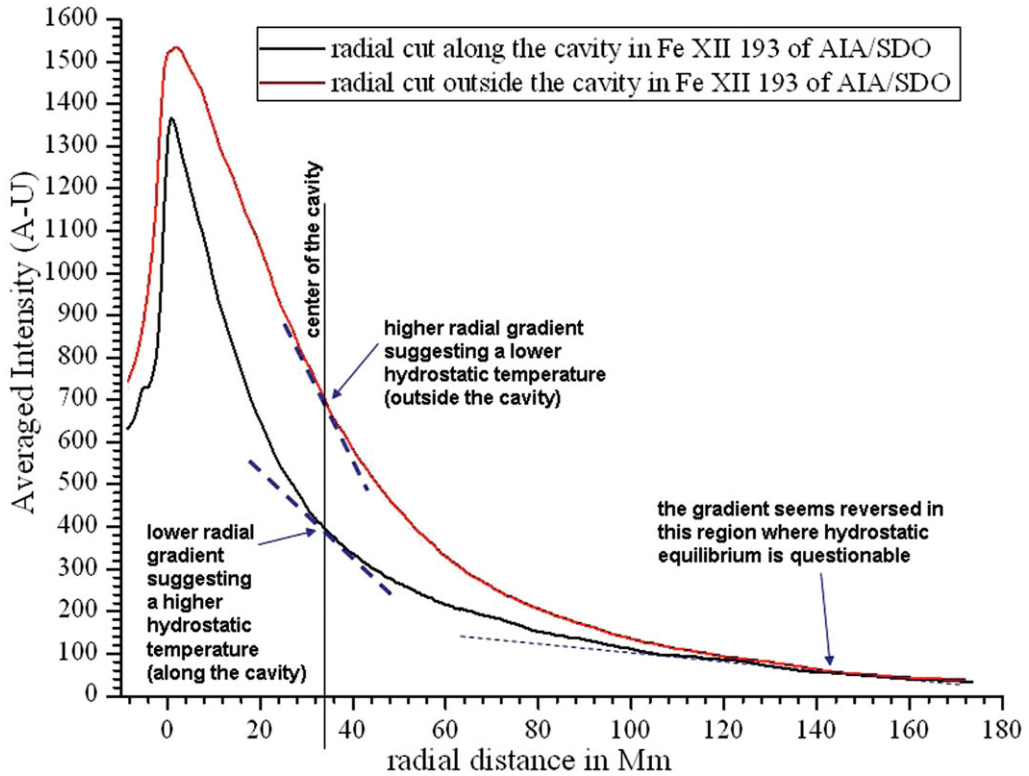


Figure 3. Averaged intensity radial cuts along and outside the south-east cavity at 138° in the 193 \AA Fe XII SDO-AIA deduced from the image shown in figure 1

4. Conclusion

Eclipse flash spectra permit to probe the deep solar interfaces without any parasitic light for evaluating their extension, including the temperature gradients. Eclipse observation gives snapshots and no temporal coverage. Unfortunately, the $P\alpha$ He II line cannot be observed near the limb outside of eclipse conditions, see Worden Beckers and Hirayama (1973). The enhancement of heating in the Fe XII 193 \AA cavity compared to the surrounding corona is in agreement with the results of Habbal *et al.* (2010) coming from the analysis of eclipse filtergrams. A better spatial resolution is needed to definitely disentangle the LOS integration effect related to the density irregularities. Visible and EUV results seem compatible but their combined analysis to study the temperature gradients is beyond the scope of this contribution.

References

- Bazin, C. Koutchmy, S., & Tavabi, E. 2012, *Solar Physics*, 286, 255
 Bazin, C. & Koutchmy, S. 2013, *Journal of Advanced Research*, 4, 307
 Cheimets, P. Caldwell, D. C. Chou, C. *et al.* 2009, *Solar Physics and Space Instrumentation III*, Proc. SPIE 7438, 14
 Habbal, S. R. Druckmuller, M. Morgan *et al.* 2010, *Astrophysical Journal*, 719, 1362
 Hirayama, T. & Irie, M. 1984, *Solar Physics*, 90, 291
 Labrosse, N. Schmieder, B. Heinzel, P. *et al.* 2011, *Astronomy and Astrophysics*, 531, 69
 Vial, J.-C. Koutchmy, S. *et al.* 1992, *ESA SP 344*, 87
 Worden, S. P. Beckers, J. M., & Hirayama, T. 1973, *Solar Physics*, 28, 73